Study of the operating conditions of radial compression columns in preparative chromatography

Matilal Sarker[a,b], Tong Yun[a,b], Georges Guiochon[a,b,*]

[a] *Department of Chemistry, The University of Tennessee, Knoxville, TN 37996-1600, USA*
[b] *Division of Chemical and Analytical Sciences, Oak Ridge National Laboratory, Oak Ridge, TN 37831, USA*

Abstract

Performance and stability were tested for radial compression columns packed with spherical particles of an octadecyl bonded silica. The performance of the radial columns remained unchanged after approximately 500 h of constant use, including a number of solvent gradient runs. The performance of analytical columns packed with the same material was comparable to that of the radial columns. The column permeability decreases and the inlet pressure required to maintain a constant flow-rate increases with increasing radial compression pressure. Maximum column efficiency was obtained for a value of radial compression pressure approximately equal to 25 bar.

Keywords: Preparative chromatography; Columns, radial compression; Radial compression columns

1. Introduction

Preparative high-performance liquid chromatography is an important tool for the purification of fine chemicals and pharmaceuticals which in recent years has found a broad field of application [1,2]. The most desirable properties of a chromatographic column are long-term stability and high efficiency. Because of improvements in the packing technology and of the experience acquired over 30 years, excellent analytical columns have become easily available. By contrast, the scaling-up of column packing from an analytical to a preparative/production level is still poorly understood. Widely different performances can be obtained with the same packing material, handled in ways which are apparently quite similar. The degree of consolidation of the column bed and

its radial homogeneity are probably the missing link between column packing and performance in preparative scale chromatography [3,4]. Their importance is demonstrated by the success of packing compression devices.

The two main types of such devices used in preparative scale chromatography are the axial (ADC) and radial (RDC) dynamic compression columns. In ADC, the stationary phase is placed inside a giant syringe whose piston is constantly pressed against the packing [5–8]. RDC is made up of plastic tubing filled with the packing and placed in the center of a steel chamber [9,10]. The packing is compressed by pumping a liquid between the plastic tube and the steel wall. Sarker and Guiochon have demonstrated that both technologies prevent the formation of any voids and cause the sealing of cracks easily formed as a result of what would normally be considered as mishandling of the columns [8,10]. As a result, the stability of the columns

---

* Corresponding author. Address for correspondence: Department of Chemistry, University of Knoxville, TN 37996-1600, USA.

is assured. With dynamic compression columns it is also possible to avoid the formation of voids at the column inlet. The origin of this nagging problem has been long ignored. It has been suggested recently that it is due to the consolidation of the column bed under external compression stress (ADC or RDC) or the viscous friction of a fast mobile phase [3,4].

The scientific literature on preparative chromatography contains relatively few papers dealing with experimental problems of an instrumental nature in which columns of internal diameter in excess of 2.5 cm are studied. The cost of the equipment needed and of the chemicals required to run experiments is nearly prohibitive for research institutes, while few engineers in industry have the time and opportunity to carry out systematic experiments. Most of the work available using RDC columns was published by Carta and Stringfield [11]. Their most important contribution is the derivation of a correlation (discussed later in this work) between the radial compression applied to the column and the inlet pressure required to maintain the mobile phase flow-rate constant. In a previous study [10], we demonstrated the efficiency and stability over a period of several hundred hours of RDC columns packed with irregularly shaped particles. Like Carta and Stringfield [11], we observed that increasing the radial compression pressure causes an increase of the inlet pressure at constant flow-rate.

The goal of this work is to investigate in detail the stability of radial compression columns packed with spherical particles and of the relationships between their performance and the operating conditions.

2. Experimental

2.1. Chemicals

All chemicals used in this work were >99% pure. Acetone, m-cresol, phenol, and methanol were purchased from Baxter (Atlanta, Georgia, USA). Phenethyl alcohol was purchased from Fluka Chemie (Switzerland). Distilled water was obtained from the still of the Chemistry Department. It was filtered before use.

2.2. Solvent

In some experiments 99.9% pure methanol was used as the solvent, a 40:60 methanol–water (v/v) mixture in others. In the following, we refer to pure methanol as 'solvent A' and to the 40:60 methanol–water mixture as 'solvent B'. For economical reasons, neither of these solvents was HPLC grade. They were recycled through the column as previously explained [8,10]. The methanol used in the analytical systems was HPLC grade.

2.3. Column

Two 17.5×7.5 cm radial compression cartridges were obtained from Biotage (Charlottesville, VA, USA). These cartridges were packed with Hyperprep C_{18}-bonded, 120-Å spherical silica. The product specifications provide for an average particle size of 12.0 μm. Several analytical columns were packed in this laboratory using the same stationary phase, and a conventional slurry packing method at 483 bar.

2.4. Instrumentation

A Kiloprep 100 HPLC pump and a Kiloprep 100 radial compression module were obtained from Biotage. The pump is capable of delivering up to 500 ml/min at a maximum pressure of 138 bar. The column inlet pressure was monitored using a Model PX603-2KG5V pressure transducer from Omega (Stamford, CT, USA). This transducer gives a 1 to 5 V (d.c.) output. To be able to use it with our data system, the output was attenuated to 0.405–2.202 V (d.c.) for a pressure between 0 and 138 bar. The dead volume of the transducer was decreased by adding Teflon packing inside the sensor head connector. The analytical system consisted of a Waters HPLC pump Model 510 and a Spectraflow Model 757 detector.

2.5. Detector

A Model 204 UV–Vis detector (Model 203-7083, Linear Scientific, Reno, NV, USA), equipped with a variable-pathlength preparative cell was used in this work. Because short pathlengths can be used, the

response of this detector remains linear up to much higher concentrations than that of conventional HPLC detectors. The cell is rated up to a flow-rate of 500 ml/min and a pressure of 150 bar.

2.6. Data acquisition

The data system consisted of a Waters System interface module with two A/D convertor boards (Milford, CT, USA). These boards permit the simultaneous monitoring of four detectors. A Waters Maxima 820 version 3.3 software was used to collect the data. The data files were uploaded to the computer network of the University of Tennessee Computer Center. For further manipulation of these data, several DOS- and VMS-based softwares in BASIC and FORTRAN were developed in this laboratory.

2.7. Methods

In most experiments, the radial compression pressure was set at 15.5 bar while there was no mobile-phase flow-rate through the column and the compression chamber was sealed, leaving the compression pressure to rise with increasing inlet pressure and mobile-phase flow-rate. In some experiments (e.g., influence of compression pressure on the flow-rate), the compression pressure was set independently and controlled.

For the low concentration experiments (e.g., HETP determinations), solvents A and B were used successively as eluent. During all experiments, the mobile phase flow-rate was measured with appropriately graduated measuring cylinders. The samples for these experiments consisted of acetone (1.6 ml/l), phenol (0.5 g/l) and m-cresol (0.6 g/l) dissolved in the eluent. Sometimes a dilute solution of phenethyl alcohol (0.2%) was also used as the sample. The sample loop volume for these injections was 1.5 ml on the preparative column and 20 μl on the analytical column (ratio 75, ratio of the columns cross-section area 118).

The data collected by the Maxima 820 was translated into ASCII format for further use. All detector outputs digitized and recorded by Maxima were in terms of volts. These voltages were con-

verted to the specific units by calibrated correlations. Several programs were written in BASIC to convert data. One of these programs calculates the column efficiency, using different equations among those suggested in the literature. The efficiency reported in this work was derived from the peak width at half height. In all sets of experiments the reduced velocities and reduced plate heights were calculated. These data were fitted to the Van Deemter equation [12] by a non-linear regression. The parameters are reported in Table 1.

3. Results and discussion

The two RDC cartridges were packed and tested by Biotage, using methanol as solvent and acetone dilute in methanol as sample. Efficiencies of 4621 and 3985 plates, respectively, were reported for the two cartridges at approximately 150 ml/min (ν = 3.15, h = 3.67 and ν = 3.96, h = 3.66, respectively). In our laboratory, under similar conditions, the efficiencies of these cartridges were 4743 and 4210 plates, respectively. These results are considerably improved over those previously reported [10]. The long-term testing of the column performance was carried out using the same experimental protocol as in our previous work [10]. The columns were first used with methanol as the solvent, later with a solution of 40% methanol in water.

3.1. Results obtained with methanol as solvent

The RDC and analytical columns were tested first for 40–50 h using methanol as the eluent and a 0.16% acetone solution in methanol as the probe. Some experiments were done with a 1% solution of phenethyl alcohol as sample, as shown in Table 1. Acetone is considered unretained in methanol and its retention time was used as column hold-up time.

Fig. 1 compares representative HETP plots obtained for acetone with the two RDC and one analytical column, all packed with the same material. The two radial columns have excellent performance. They are very similar but quite different from the analytical column. As previously reported [10], the

Table 1
Van Deemter parameters for the radial and analytical columns (with $b = 1.80$)

Column No.	Solvent	Sample	a	c	h_{min}	ν_{opt}	Hours used
Analytical 1	A	Acetone	2.94	0.16	4.01	3.37	
Analytical 1	A	Acetone	2.08	0.33	3.61	2.35	
Analytical 1	A	Phenethyl alcohol	2.93	0.15	3.96	3.51	
Radial 4	A	Phenethyl alcohol	2.44	0.07	3.16	5.05	5
Radial 4	A	Acetone	3.16	0.02	3.55	9.15	38
Analytical 3	A	Phenethyl alcohol	1.09	0.17	2.19	3.27	
Radial 4	B	Phenethyl alcohol	2.47	0.03	2.96	7.39	74
Analytical 3	B	Phenethyl alcohol	1.59	0.05	2.19	6.02	
Analytical 3	B	Phenethyl alcohol	1.81	0.05	2.39	6.19	
Analytical 5	B	Phenethyl alcohol	2.05	0.50	3.94	1.90	
Radial 4	B	Acetone	3.42	0.42	5.16	2.07	140
		Phenol	2.88	0.03	3.37	7.39	
Radial 4	B	Acetone	3.60	0.06	4.23	5.72	159
		Phenol	3.48	0.02	3.84	9.95	
Radial 4	B	Acetone	2.93	0.13	3.90	3.72	262
		Phenol	2.94	0.07	3.62	5.26	
		Cresol	3.49	0.04	4.04	6.55	
Radial 4	B	Acetone	4.66	0.02	5.08	8.66	270
		Phenol	3.17	0.05	3.77	6.00	
		Cresol	3.40	0.04	3.92	6.88	
Radial 4	B	Acetone	4.23	0.02	4.63	9.05	323
		Phenol	3.57	0.03	4.03	7.88	
		Cresol	2.59	0.09	3.41	4.40	
Radial 4	B	Acetone	5.28	0.01	5.50	16.0	333
		Phenol	3.61	0.03	4.07	7.88	
		Cresol	3.59	0.02	3.70	9.49	
Radial 4	B	Acetone	5.67	0.07	6.37	5.18	483
		Phenol	3.94	0.02	4.35	8.85	
		Cresol	4.13	0.01	4.32	19.0	
Radial 5	A	Acetone	2.54	0.06	3.22	5.30	29
Radial 5	A	acetone	2.92	0.04	3.44	6.88	48
Radial 5	B	Acetone	4.65	0.01	4.93	12.8	156
		Phenol	2.93	0.02	3.33	9.05	
		Cresol	2.49	0.03	2.92	8.32	
Radial 5	B	Acetone	2.85	0.05	3.42	6.33	
		Phenol	2.85	0.03	3.30	8.02	
		Cresol	2.36	0.04	2.88	6.98	
Analytical 5	B	Acetone	1.82	0.07	2.52	5.11	
		Phenol	1.74	0.06	2.41	5.35	
		Cresol	2.12	0.05	2.71	6.06	

Solvent A=100% methanol.
Solvent B=40:60 methanol–water (v/v).

value of c is much lower for the RDC than for the analytical column (Table 1).

3.2. Results obtained with 40:60 methanol–water as solvent

The RDC columns were tested for 500 and 210 h, respectively. The columns were tested several times by determining an HETP curve. The data were fitted to the Van Deemter equation [12], assuming a value of 1.8 for the coefficient b, because of the lack of a sufficient number of data points at low flow-rates. The best values of the parameters are included in Table 1. From this table it is clear that both RDC columns performed well until the end of this prolonged use.
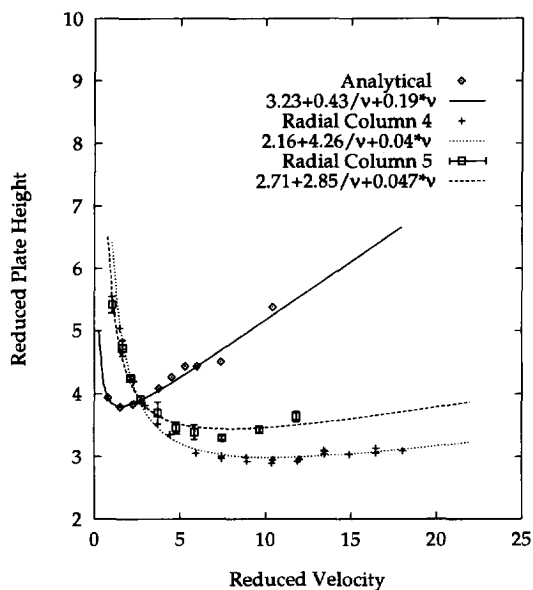
Fig. 1. Plot of reduced plate height versus reduced velocity for radial compression and analytical columns. Solvent was 100% methanol, and the sample was 1% acetone. Lines are fitted data to the Van Deemter equation. For radial column no. 5 the standard deviation was measured by injecting three to five times at each flow-rate. The solid lines are the data fitted to the Van Deemter equation.
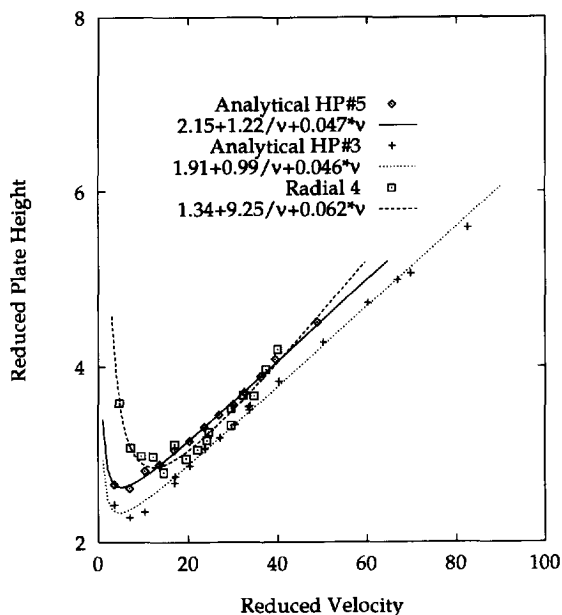

Fig. 2. Plot of reduced plate height versus the reduced velocity for the radial and analytical columns. The solvent is methanol–water (40:60, v/v), and the sample is phenethyl alcohol in the solvent. The lines are the data fitted to the Van Deemter equation.

Fig. 2 shows the HETP curves for phenethyl alcohol ($k' = 4.7$). By contrast with Fig. 1, the slopes of the HETP curves obtained with the RDC and the analytical columns are similar, with a slightly better efficiency for the analytical columns than for the RDC column. The values of a, c, h_{min}, and ν_{opt} listed in Table 1 for the RDC and the first two analytical columns are very close, although the dimensions of these two analytical columns are different (15×0.46 cm and 25×0.46 cm).

3.3. Correlations between column inlet pressure, compression pressure, and flow-rate

Under the standard operation procedure of the radial compression columns, the radial compression stress is preset (at 15.5 bar) before starting the pumping of the mobile phase through the column. As a result, the radial compression stress of the column bed increases with increasing flow-rate. Thus, the flow-rate depends on the inlet pressure, on the radial compression stress and on the previous history of the

column: we have shown [3,4] that there is no reversibility in packing consolidation. As long as there is positive compression stress the packing rebound resulting from a stress reduction is very small. A negative stress causes a catastrophic failure of the bed, cracks form and column efficiency is lost; this phenomenon has been discussed [10] and is no longer considered here. The investigation of the relationship between flow-rate, radial compression stress and inlet pressure has been pursued.

Constant volume of compression fluid

The consolidation of the column under this radial stress increases progressively. It seems that it does so more slowly than with axial compression columns. The measurement of the length of an ADC column after the compression stress has been increased sharply, shows a progressive reduction of this length which stabilizes after a time which depends on the nature of the packing and varies between 10 h for an irregularly shaped particle material and 8 to 60 min for two spherical particle materials. As illustrated in
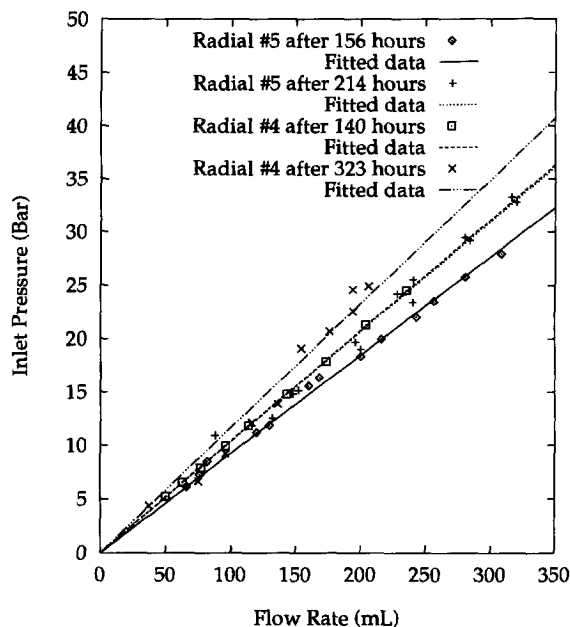
Fig. 3. Plot of inlet pressure at different flow-rates for the radial columns after different periods of use. All data have been corrected for the system pressure. The solvent was methanol–water (40:60, v/v). Solid lines are the linear regression lines passing through the origin.

Fig. 3, which shows plots of the head pressure versus the mobile phase flow-rate (solvent B), the column permeability decreases slowly with passing time, by approximately 10% over a period of several hundred hours. The duration of the experiment was insufficient to suggest whether a stable bed was achieved or, if not, when it would have been. A parallel

reduction in the column porosity was observed (Table 2). The initial porosity of RDC column no. 4 was lower than that of RDC column no. 5. Note that we have not observed this slow decrease of the column permeability with ADC columns [8,13]. It may result from the different distribution of compression stress in an ADC and an RDC column. With an RDC column, the volume available to the packing material remains constant because the compression chamber is closed. The increase in compression pressure results from the increase in the reaction of the mobile phase against the cartridge wall. We can consider the total stress applied to the packing itself as constant, although is may vary locally.

The permeability derived from the data in Fig. 3 was used to estimate the hydrodynamic average particle size, using the correlation classical in chromatography, $\Delta P = (u \eta L \phi)/d_p^2$ with ΔP=head pressure, d_p=average particle size, u=average mobile-phase velocity, η=mobile-phase velocity, L=column length, and $\phi = 500$ for spherical particles. The average particle sizes obtained for column no. 5 after 156 h and 214 h of use were 9.09 and 8.64 μm, respectively. For column no. 4, after 140 and 323 h of use, this size was 8.67 and 8.31 μm, respectively. These observations are in agreement with our previous results from the consolidation of stationary phases in ADC and RDC columns [8,10] and from work on the fundamentals of consolidation of packed beds [3,4]. They are explained by the reduction of the external porosity of the column bed. The actual particle size remains constant; no or very few

Table 2
Column characteristics

Characteristics	Analytical column 1	Analytical column 2	Radial column 4	Radial column 5
Column dimension (cm)	25.0×0.46	15.0×0.46	17.5×7.5	17.5×7.5
Dead volume, solvent A (cm^3)	2.95±0.09	not done	563	568
Phase ratio, solvent A	0.38±0.04	not done	0.38	0.36
Total porosity, solvent A	0.71±0.02	not done	0.73	0.74
Dead volume, solvent B (cm^3)	2.82±0.09	1.70	532±2	543
Phase ratio, solvent B	0.47±0.05	0.47	0.47±0.02	0.43
Total porosity, solvent B	0.68±0.02	0.68	0.68±0.01	0.71
k' (Acetone)	0.26±0.01	not done	0.28±0.01	0.28±0.03
k' (Phenol)	2.53±0.08	not done	1.98±0.14	1.94±0.10
k' (Cresol)	5.81±0.21	not done	4.73±0.17	4.37±0.22
k' (Phenethyl alc.)	4.63±0.11	4.57±0.04	3.82±0.05	not done

Solvent A=100% methanol.
Solvent B=40:60 methanol–water (v/v).

particles are broken under the rather moderate level of compression stress applied [4].

Inlet pressure measured at constant radial compression stress

In this set of experiments the radial compression stress applied is kept constant (at 20.7 bar) while the inlet pressure is increased and the flow-rate measured. Fig. 4 shows the plot of inlet pressure versus flow-rate. From the slope the permeability is calculated. It should be noted here that, in this experiment, the effective radial stress applied to the column packing decreases with increasing head pressure because the stress applied by the mobile phase as a result of the integral of the influence of its pressure on the whole cartridge increases with increasing head pressure while the compression pressure remains constant. The effective stress results from the combination of the external stress and the stress applied by the mobile phase. Nevertheless, the permeability of the column has hardly changed compared to the value obtained in the previous experiment. This confirms the small elasticity of the packing previously reported.

Effect of the radial compression on the inlet pressure

Fig. 5 illustrates the correlation between the radial compression and the inlet pressure. In this set of experiments the flow-rate was kept constant at 118 ml/min. The radial compression was set each time while no liquid was being pumped through the column. The inlet pressure remains approximately constant as long as the compression stress is below 20 kg/cm^2. This is easily explained by the fact that after several hundred hours of operation the packing was well consolidated for the stress corresponding to an initial pressure of 15.5 atm (see operating procedure). For higher stress, the data in Fig. 5 show that the inlet pressure increases in a nonlinear fashion with increasing radial compression stress. The data fit well to a second degree polynomial. The inlet pressure increases from 14.2 bar to 16.7 bar when the radial compression stress increases from

Fig. 4. Plot of inlet pressure at different flow-rates while the radial compression pressure was kept constant (20.7 bar). The solid line is the linear regression line passing through the origin. The solvent in all experiments was methanol–water (40:60, v/v).
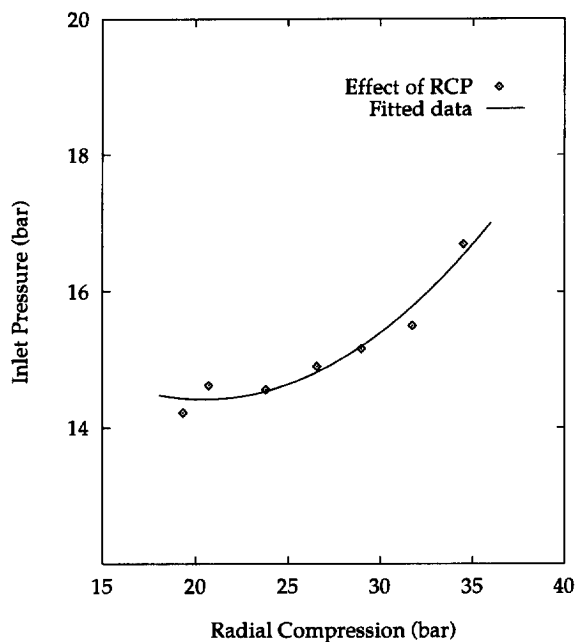

Fig. 5. Effect of radial compression on inlet pressure for the radial compression column no. 4. The flow-rate was constant at 118 ml/min in all experiments. The solvent was methanol–water (40:60, v/v).

19.3 to 34.5 bar: a 17.5% increase of the inlet pressure for a 79% increase of the radial compression stress. This increase is explained by the rapid decrease of the bed permeability with decreasing external porosity of the column. The rate of increase of the inlet pressure is steeper than the one found in a similar experiment performed previously with irregular particles [10]. This result is in agreement with the independent observation that materials made of spherical particles consolidate to a greater extent under moderate compression stress than those made of irregularly shaped particles [4].

Fig. 6 shows a plot of the radial compression stress actually measured under steady state conditions versus the set radial compression stress. The actual pressure of the compression fluid is always higher than the set pressure because of the interaction with the pressurized mobile phase inside the column.

Permeability versus radial compression

The column permeability decreases linearly with increasing radial compression stress, as shown in Fig. 7. This result is in agreement with previous

findings obtained with irregularly shaped particles [10], as explained above.

3.4. Effective radial compression

Under standard operating conditions, the compression fluid is pumped into the compression chamber until a certain pressure is reached while there is no mobile phase flow along the column. Then, the valve at the entrance of the compression chamber is closed, confining the compression fluid inside the chamber. When pumping of the mobile phase through the column begins, the pressure of the solvent inside the column increases and acts against the radial compression of the cartridge wall. The local pressure inside the column decreases almost linearly with increasing distance from the inlet. As a result, the effective stress applied to the cartridge wall is directed toward the outside of the column near the entrance and is zero at a distance L' approximately equal to $L(1 - P_{rcp}/P_i)$, where L is the column length and P_{rcp} the compression pressure measured when the inlet pressure is P_i (if $L' < 0$, the whole bed is under positive effective compression stress). Closer to the column outlet, the effective stress is
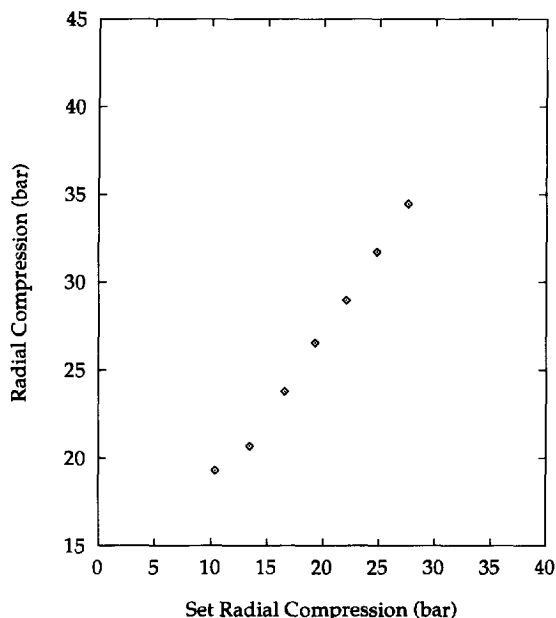

Fig. 6. Correlation between the set radial compression at zero flow-rate and the measured radial compression. The flow-rate constant at 118 ml/min.
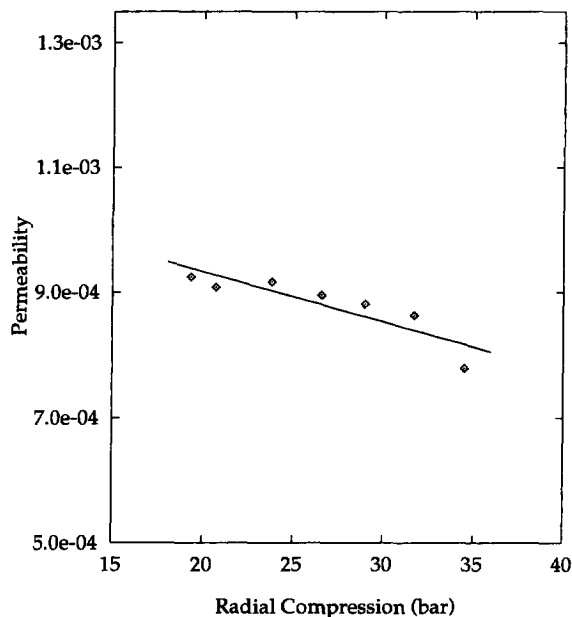

Fig. 7. Dependence of column permeability on the radial compression pressure for radial column no. 4.

directed toward the inside of the column. So, the cartridge tends to be inflated at the column entrance and compressed at its exit. However, whatever the inlet pressure and the pressure distribution along the cartridge wall, the volume of liquid inside the compression chamber is constant, and thus the internal volume of the cartridge is also constant [11]. Therefore, a change in the head pressure tends to produce a redistribution of the packing density along the column. Because particles move with difficulty, if at all, this causes local changes in the packing density, which may explain the dependence of column efficiency on the compression pressure (see next section). Spherical particles tend to move more easily than irregularly shaped ones, and a redistribution of the material when the compression stress is changed cannot be ruled out.

Carta and Stringfield [11] have derived an empirical relationship between the column inlet pressure and the effective radial compression, defined as the difference between the measured radial compression and the column inlet pressure

$$P_{rcp} - P_i = P^0_{rcp} - \frac{1}{2}P_i \qquad (1)$$

where P^0_{rcp} is the set radial compression at zero flow-rate. Fig. 8 compares the plots of the effective radial compression versus the measured inlet pressure predicted by Eq. 1 (solid line) and resulting from the data obtained with the two cartridges (symbols). For some unknown reason, the agreement between predicted and measured data is much better for cartridge 5 than for 4. A large part of the scatter of the experimental data is due to the lack of precision in the reading of the radial compression pressure. Fig. 9 shows a plot of the initial radial compression pressure required to achieve a constant effective compression pressure versus the flow-rate. In this experiment the radial compression pressure set at zero flow-rate (P^0_{rcp}) was varied in order to achieve a constant effective radial compression. As indicated by Eq. 1, this plot should be a straight line. The experimental data are in excellent agreement with this prediction.

The simple approach followed by Carta and Stringfield accounts for most of the effect observed in Fig. 8 and for the experimental results in Fig. 9. However, some question remains as to whether both
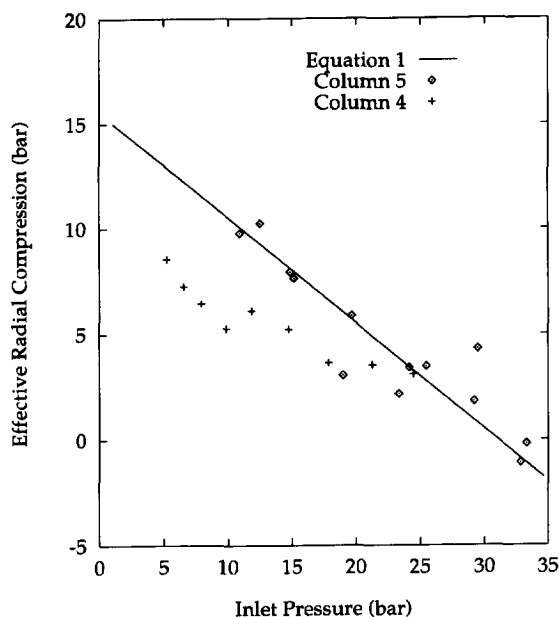

Fig. 8. Plot of effective radial compression versus the inlet pressure of radial column no. 5. The solvent was methanol–water (40:60, v/v). The set radial pressure at flow was 15.5 bar. The solid line is the plot of Eq. 1.
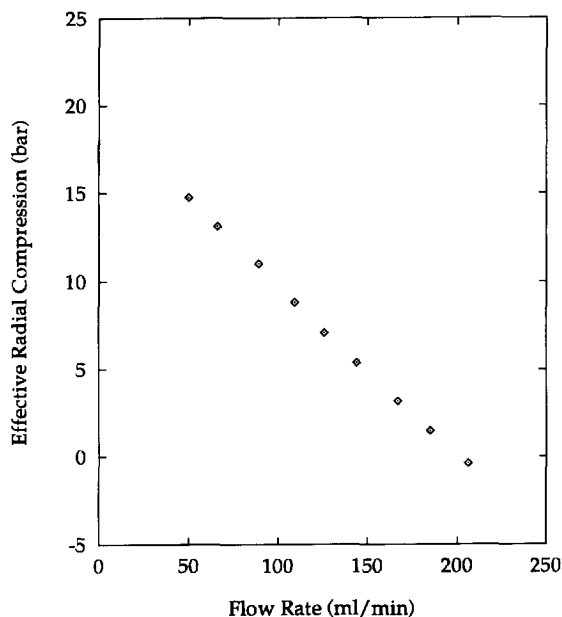

Fig. 9. Plot of effective radial compression versus the flow-rate at a constant radial compression pressure.

the total column volume and the volume confined inside the chamber remain constant during operation (their sum is certainly constant). The constancy of the two volumes requires that we neglect the influence of the rigidity of the cartridge wall and assumes that the packing density is constant and that the compression stress is isotropic. Most probably these assumptions are not valid; the packing density, which varies with the position in the column, depends also on the history of bed consolidation. A more detailed analysis requires that progress be made regarding our understanding of the behavior of packing materials under compression stress, a phenomenon which is not yet fully understood. The planar geometry of the compression stress distribution in an ADC is, in principle, much simpler than the cylindrical geometry of this stress in an RDC, but the interference of the bed friction against the wall introduces other kinds of complexity. Its analysis, which is necessary for further progress in the performance of chromatographic columns, will require considerable efforts.

3.5. Effect of the radial compression on the column efficiency

In this set of experiments the flow-rate was kept constant at 118 ml/min while the radial compression was increased. Several injections of a dilute solution of acetone and phenol were made at each value of the radial compression pressure. The results are plotted in Fig. 10. When the radial compression stress increases, we observe a slight increase of the reduced plate height for acetone and a nearly constant reduced plate height for phenol. This result, which confirms our previous findings [10], suggests that too high a degree of consolidation by radial compression tends to increase the disorder of the packing and to decrease its homogeneity.

4. Conclusion

For obvious reasons, our results have been acquired using only a limited number of columns. Thus, our conclusions should be considered as somewhat preliminary. However, the results of the experiments performed are consistent with our own previous results [10] and those of Carta and Springfield [11]. Furthermore, like these previous results, they are in full agreement with all that we know at this stage on the consolidation of pulverulent materials. Therefore, they should be considered most seriously by those active in the field.
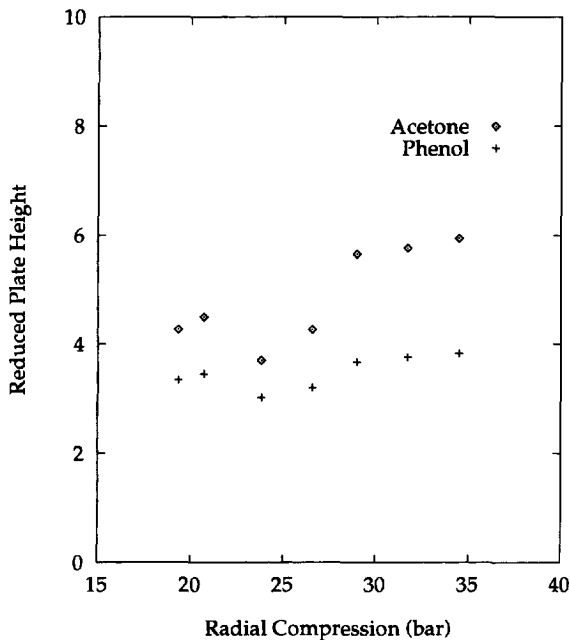

Fig. 10. Effect of radial compression on the efficiency of columns. The solvent was methanol–water (40:60, v/v), and the sample was acetone and phenol in the solvent. The flow-rate was constant at 118 ml/min.

Kiloprep 100 radial compression module, and the Linear Scientific preparative UV detector.

References

[1] M. Verzele, M. De Conick, J. Vindevogel and C. Dewaele, J. Chromatogr., 450 (1988) 47.

[2] M. Verzele and C. Dewaele, Preparative High Performance Liquid Chromatography, TEC, Gent, 1986, Chap. I.

[3] G. Guiochon and M. Sarker, J. Chromatogr. A, 704 (1995) 247.

[4] M. Sarker, A.M. Katti and G. Guiochon, J. Chromatogr. A, 719 (1995) 275.

[5] E. Godbille and P. Devaux, J. Chromatogr., 122 (1976) 317.

[6] H. Colin, P. Hilaireau and J. de Tournemire, LC·GC, 8(4) (1990) 302.

[7] D.-R. Wu and K. Lohse, J. Chromatogr. A, 658 (1994) 381.

[8] M. Sarker and G. Guiochon, J. Chromatogr. A, 702 (1995) 27.

[9] J.N. Little, R.L. Cotter, J.A. Prendergast and P.D. McDonald, J. Chromatogr., 126 (1976) 439.

[10] M. Sarker and G. Guiochon, J. Chromatogr. A, 683 (1994) 293.

[11] G. Carta and W.B. Stringfield, J. Chromatogr. A, 658 (1994) 407.

[12] J.J. Van Deemter, F.J. Zuiderweg and A. Klinkenberg, Chem. Eng. Sci., 5 (1956) 271.

[13] M. Sarker and G. Guiochon, J. Chromatogr. A, 709 (1995) 227.